

Supporting Information

A ‘smart’ aptamer-functionalized continuous label-free cell catch-transport-release system

*Bozhen Zhang, ‡^a Canran Wang, ‡^a Yingjie Du^a, Rebecca Paxton^b and Ximin He^{*a}*

^a Department of Materials Science and Engineering, University of California, Los Angeles, CA 90095, USA

^b University of Arizona College of Medicine – Phoenix, Phoenix, AZ 85004, USA

‡ These authors contributed equally

* Corresponding author. Email: ximinhe@ucla.edu

Table of contents

Note S1 Discussion on the responding sequence of aptamer and hydrogel.

Note S2 Derivation of the system throughput.

Table S1 Sequences of the cell-catching aptamers and scrambled control.

Fig. S1 The XPS result of pure PNIPAAm.

Fig. S2 The thermal-responsive shrinking and swelling property of aptamer-functionalized PNIPAAm.

Fig. S3 Quantification of cell catching capability of PNIPAAm hydrogels with different aptamers.

Fig. S4 Microscopic images and quantification of cells remaining on the aptamer-functionalized hydrogel after different operations.

Fig. S5 Quantification of cells attachment density on pure PNIPAAm hydrogel at RT and 45°C.

Video S1 The swelling and shrinking process of aptamer-PNIPAAm in response to temperature changes.

Video S2 The cell releasing process triggered by 45 °C water of an iCatch microfluidic device with caught CCRF-CEM cells.

Note S1 Discussion on the responding sequence of aptamer and hydrogel.

The cell releasing process of the iCatch system relies on the sequential response to heating of the hydrogel and aptamer. The responding rates of these two components are within a close range and our design prevents the aptamers on the upper surface of the hydrogel to reach the warm buffer before the hydrogel contracts, which ensures this sequence when warm buffer is pumped into the lower channel of the device.

To compare the responding rates of the hydrogel and aptamer, we estimate the $\tau_{1/2}$ of contraction of the hydrogel and denaturation-induced cell release of the aptamer. For hydrogel PNIPAAm, the kinetics of its dimensional change can be described with the following formula:¹

$$R = \frac{6R_0}{\pi^2} e^{-\frac{t}{\tau}}$$

, where R is the dimension of the hydrogel, R_0 is the original dimension of the corresponding direction, t is time of phase transition, and τ is the characteristic time of this transition, defined as^{1,2}

$$\tau = \frac{R^k}{\pi^2 D}$$

, where D is the collective diffusion coefficient and k is a factor equal to (theoretically) or slightly lower than (experimentally) 2.

The thickness of the hydrogel used in the iCatch device is around $R = 1$ mm, the k of PNIPAAm can be determined as 1.6,² and the D can be estimated as 10^{-5} cm²/s,³ thus the characteristic time τ can be estimated as $\sim 10^2$ s. Therefore, the $\tau_{1/2}$ of the hydrogel transition is estimated as

$$\tau_{\frac{1}{2}}(\text{hydrogel}) = -\tau \ln \frac{\pi^2}{12} = 19.5 \text{ (s)}$$

For the denaturation-induced cell release of aptamer, there has not been a mature model, thus we use the kinetic model of aptamer-protein complex dissociation to estimate it. According to several works,^{4,5} the dissociation is a first-order reaction and the rate constant k_{off} is around $1 \sim 10^{-3}$ s⁻¹. So the $\tau_{1/2}$ of aptamer is estimated as

$$\tau_{\frac{1}{2}}(\text{aptamer}) = \frac{\ln 2}{k_{\text{off}}} = 1 \sim 10^3 \text{ (s)}$$

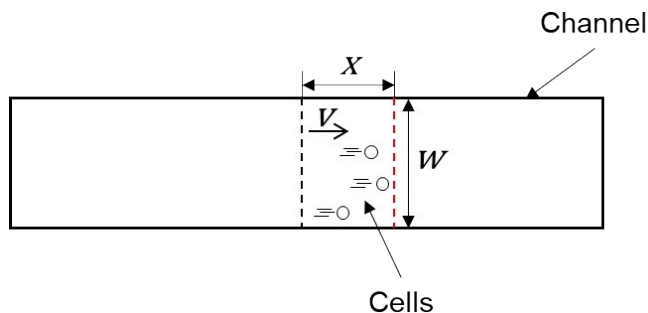
Therefore, the half-lives of hydrogel phase transition and aptamer dissociation are within a relatively similar range, which indicates that theoretically the tendency for aptamers to release the cells before the hydrogel contracts is low.

More importantly, due to the design of the microfluidic system, the warm buffer can only contact the lower part of the hydrogel at the first stage of pumping the warm buffer. Only after the hydrogel contracts and its cell-loaded top surface enters the lower channel, can the aptamers directly contact the warm buffer. And due to the limited heat transfer in the hydrogel (thermal diffusivity of $\sim 10^{-7}$ m²/s,⁶ thermal

conductivity $\sim 0.6 \text{ W}\cdot\text{m}^{-1}\cdot\text{K}^{-1}$),⁷ it is difficult for the aptamers to be heated to the critical temperature before they contact the warm buffer. Therefore, most aptamers denature to release the cells after the hydrogel contracts in a sequential manner, which prevents cells from being lost in the top channel.

Note S2 Derivation of the system throughput.

The throughput of a fluidic system can be defined as the number of items passing through a specific cross-section within a specific duration. Taking the function of the iCatch system into consideration, here we define the throughput of the system as the number of cells flowing through and captured in a unit of time and channel width (instead of cross-sectional area because the thickness of the channel is negligible compared to its length and width). To derive this throughput, we can analyze with a scheme



as below:

The number of the cells within the area defined by the dash lines is

$$N = xwC$$

, where C is the two-dimensional cell density of captured cells.

The duration for all these cells to cross the red line is

$$t = \frac{x}{v}$$

Therefore, the throughput of the system is

$$T = \frac{N}{wt} = Cv$$

, which is throughput = two-dimensional density of captured cells \times velocity.

Table S1 Sequences of the cell-catching aptamer sgc8c (A, B) and scrambled control (C). To enable the grafting of aptamer to PNIPAAm, A and C are modified with the acrydite group at their 5' ends.

Name	Sequence (5'- 3')
A	Acrydite-TTT TTT ATC TAA CTG CTG CGC CGC CGG GAA AAT ACT GTA GGG TTA GAT
B	TTT TTT ATC TAA CTG CTG CGC CGC CGG GAA AAT ACT GTA GGG TTA GAT
C	Acrydite-TTT TTT ATT ACC TCT AAA TCA CTG CTC TGT AAC ATG GTC GCG CTA GGT

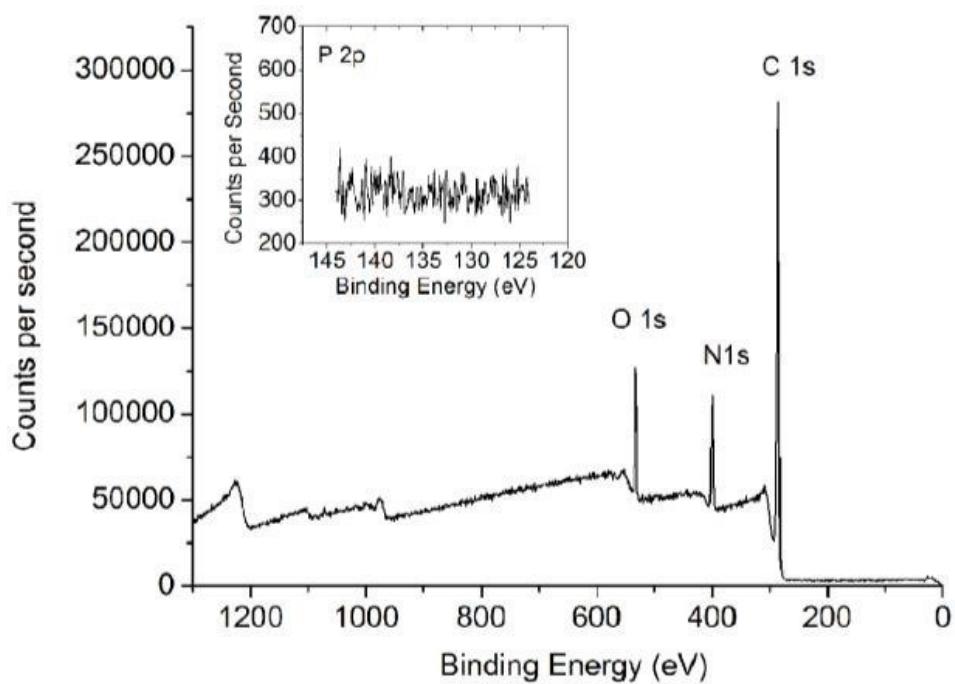


Fig. S1 The XPS result of pure PNIPAAm.

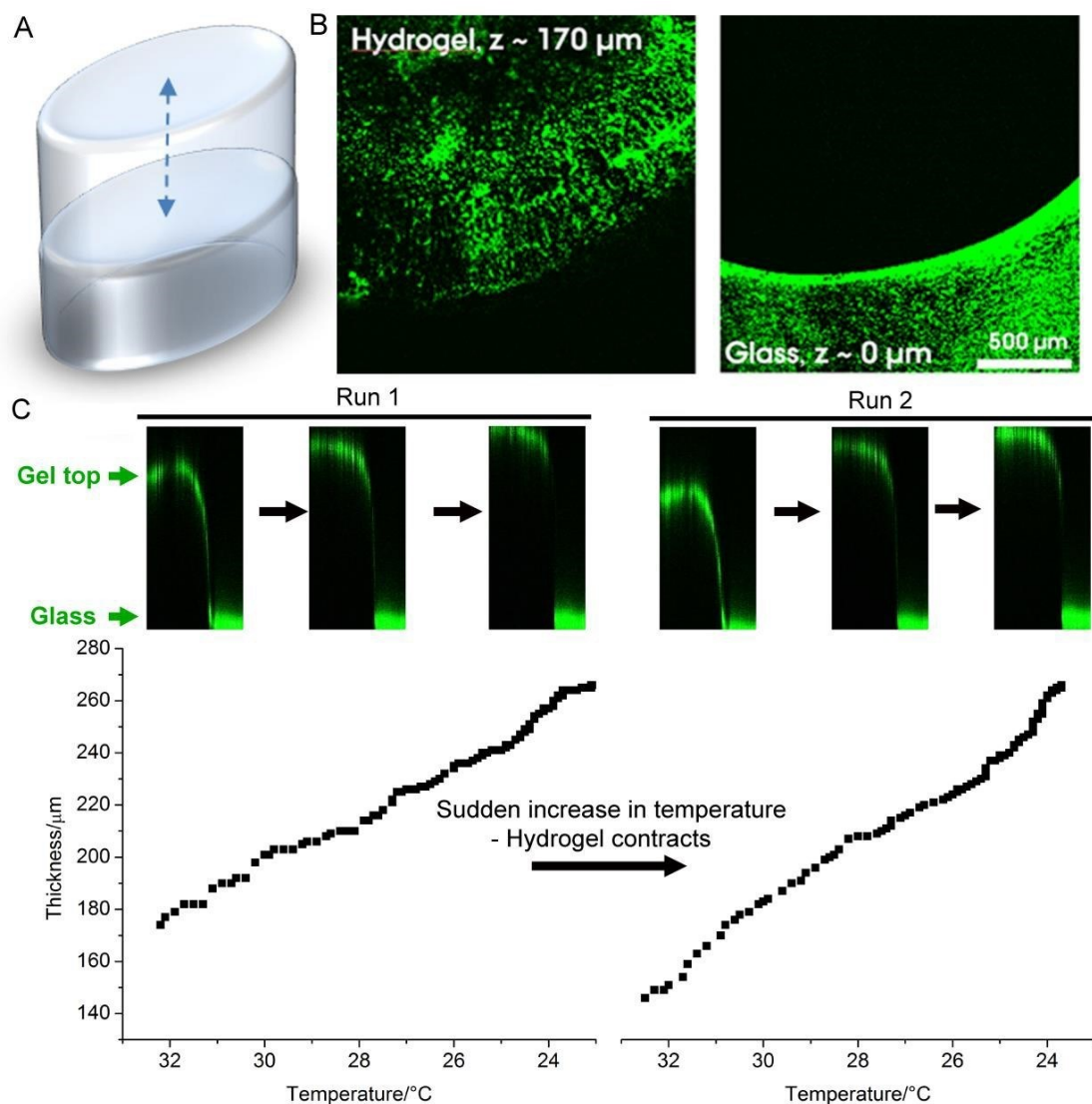


Fig. S2 The thermal-responsive shrinking and swelling property of the aptamer-functionalized hydrogel. **A.** A schema of the shrinking and swelling of the hydrogel. **B.** Confocal photos of two slices from the contracted gel ($T \sim 32^\circ\text{C}$), showing the hydrogel surface ($z = 170\ \mu\text{m}$, left) and the bottom glass slide ($z = 0\ \mu\text{m}$, right). The thickness of the hydrogel is determined by calculating the distance between the surface and the bottom. **C.** The relationship between the hydrogel thickness and the temperature in a heating-cooling cycle. It shows that the thickness of the hydrogel increases linearly from ~ 170 to $\sim 270\ \mu\text{m}$ with a rate of $\sim 12\ \mu\text{m}/^\circ\text{C}$ as the temperature drops from 32°C to room temperature. The inserts represent cross-sectional views of the hydrogel at different temperatures.

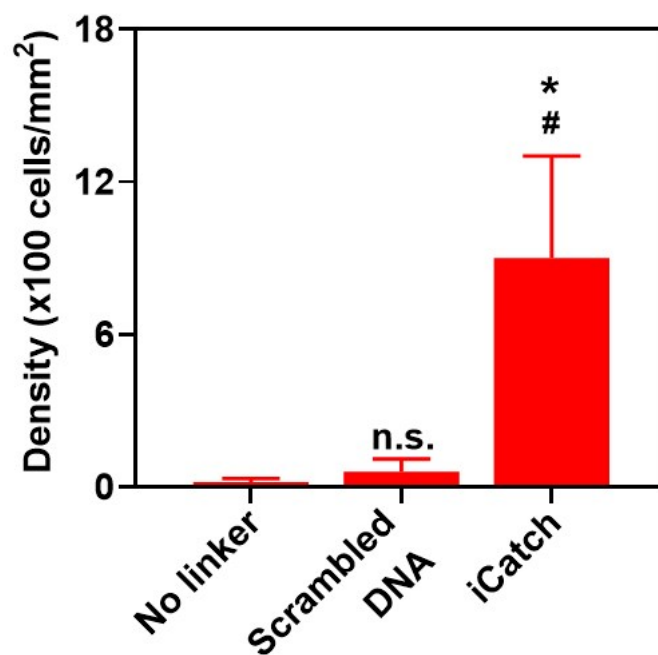


Fig. S3 Quantification of CCRF-CEM cell catching capability of PNIPAAm hydrogels synthesized with 1) sgc8c aptamer without acrydite linker for covalent binding (Sequence B in **Table S1**), 2) the aptamer with scrambled DNA sequences with acrydite linker (Sequence C in **Table S1**), and 3) sgc8c aptamer with acrydite linker designed for CCRF-CEM cell affinity (Sequence A in **Table S1**). Unpaired t test was performed for analysis. * $p < 0.05$, compared with the group without linkers. # $p < 0.05$, compared with the group with scrambled DNA.

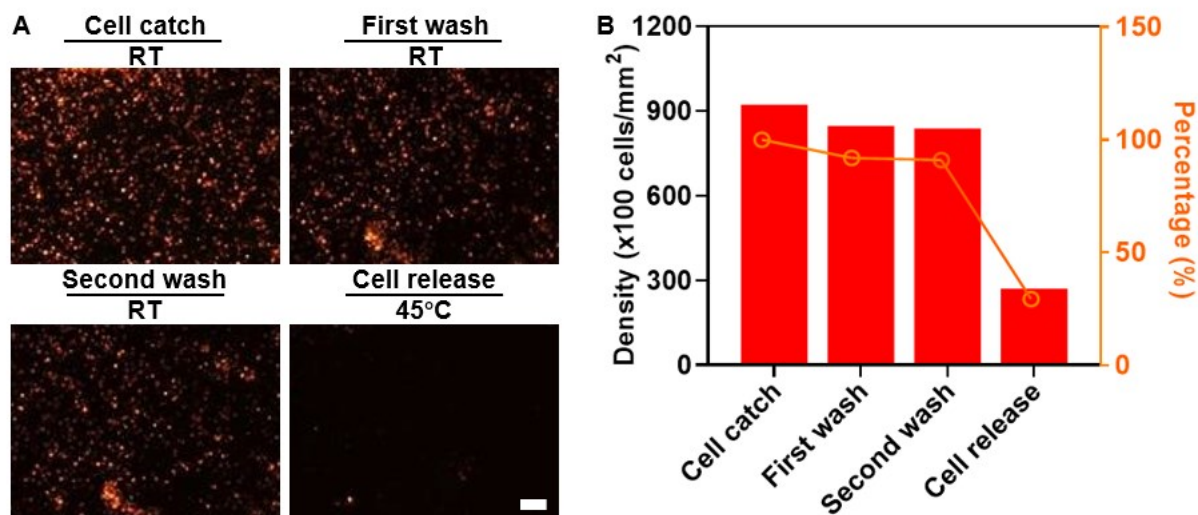


Fig. S4 A. Microscopic images of CCRF-CEM cells remaining on the aptamer-functionalized hydrogel after 1) cell catching at RT, 2) 1 wash at RT after cell catching, 3) 2 washes at RT, and 4) 1 wash at 45°C (cell release). (scale bar = 200 μ m). **B.** Quantification of cells attached to the hydrogel after each step of wash.

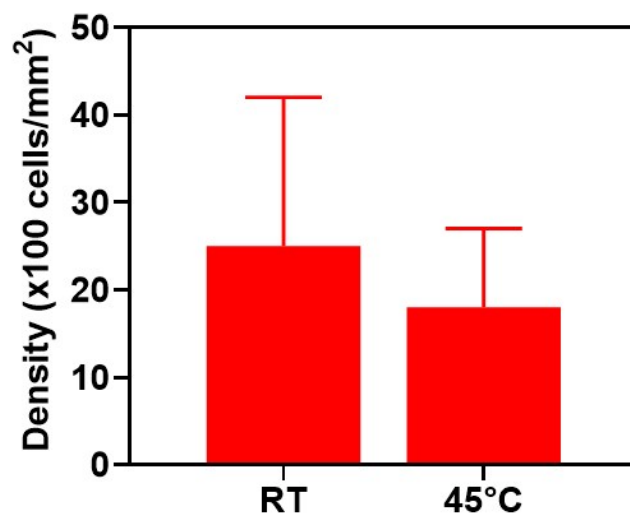


Fig. S5 Quantification of CCRF-CEM cells attachment density on pure PNIPAAm hydrogel at RT and 45 °C.

Reference

1. T. Tanaka, E. Sato, Y. Hirokawa, S. Hirotsu and J. Peetermans, *Phys. Rev. Lett.*, 1985, **55**, 2455-2458.
2. E. S. Matsuo and T. Tanaka, *J. Chem. Phys.*, 1988, **89**, 1695-1703.
3. S. M. Cho and B. K. Kim, *J. Biomater. Sci., Polym. Ed.*, 2010, **21**, 1051-1068.
4. A. T. H. Le, S. M. Krylova and S. N. Krylov, *Anal. Chem.*, 2019, **91**, 8532-8539.
5. M. Leitner, A. Poturnayova, C. Lamprecht, S. Weich, M. Snejdarkova, I. Karpisova, T. Hianik and A. Ebner, *Anal. Bioanal. Chem.*, 2017, **409**, 2767-2776.
6. A. Tél, R. A. Bauer, Z. Varga and M. Zrínyi, *Int. J. Therm. Sci.*, 2014, **85**, 47-53.
7. X. Yin, Y. Zhang, Q. Guo, X. Cai, J. Xiao, Z. Ding and J. Yang, *ACS Appl. Mater. Interfaces*, 2018, **10**, 10998-11007.